THE PROTEIN SOCIETY

FOR THE RECORD

Detection of disordered regions in globular proteins using ^{13}C-detected NMR

Felicia L. V. Gray,[1,2] Marcelo J. Murai,[1] Jolanta Grembecka,[1,2] and Tomasz Cierpicki[1,2]*

[1]Department of Pathology, University of Michigan, Ann Arbor, Michigan 48109
[2]Program in Chemical Biology, University of Michigan, Ann Arbor, Michigan 48109

Received 29 July 2012; Revised 26 September 2012; Accepted 1 October 2012
DOI: 10.1002/pro.2174
Published online 9 October 2012 proteinscience.org

Abstract: Characterization of disordered regions in globular proteins constitutes a significant challenge. Here, we report an approach based on ^{13}C-detected nuclear magnetic resonance experiments for the identification and assignment of disordered regions in large proteins. Using this method, we demonstrate that disordered fragments can be accurately identified in two homologs of menin, a globular protein with a molecular weight over 50 kDa. Our work provides an efficient way to characterize disordered fragments in globular proteins for structural biology applications.

Keywords: protein disorder; menin; structural biology; NMR spectroscopy

Introduction

Disordered regions in proteins can play important roles in protein function. These regions are frequently involved in cell signal transduction, transcriptional regulation, molecular recognition, and protein regulation through posttranslational modification.[1,2] The identification and characterization of disordered regions in proteins has become an important task for computational protein structure prediction and for structural biology.[3–6] Disordered fragments can be predicted using various bioinformatics methods[3,6,7]; however, high-resolution experimental validation and biophysical characterization of these regions remain challenging. Accurate methods for the identification of disordered fragments in globular proteins are of significant interest to the structural biology community as the presence of flexible protein segments may interfere with the production of diffraction quality crystals. Consequently, extensive protein engineering can be required to remove these flexible regions to enable crystallization or improve the quality of protein crystals. For example, the recent X-ray structure of the *Drosophila* effector caspase drICE required the deletion of a highly flexible internal fragment.[8] Additionally, deletion of internal flexible regions in the GluR2 receptor ligand-binding domain resulted in improved diffraction of protein crystals from 2.5 to 1.5 Å.[9,10] Experimental identification of internal-disordered regions is commonly based on rapid hydrogen-deuterium exchange rates for solvent-exposed amide protons, which can be detected using mass spectrometry.[11,12] Nevertheless, accurate identification of disordered residues remains difficult, and an

Additional Supporting Information may be found in the online version of this article.

Grant sponsor: American Cancer Society Research Scholar Grant; Grant number: RSG-11-082-01-DMC; Grant sponsor: NIH; Grant number: 1R01CA160467.

*Correspondence to: Tomasz Cierpicki, Department of Pathology, University of Michigan, 1150 W. Medical Center Drive, MSRB1 4516, Ann Arbor, MI 48109.
E-mail: tomaszc@umich.edu

efficient strategy to experimentally detect such fragments in globular proteins would significantly facilitate the design of protein constructs suitable for crystallization. Furthermore, identification of disordered residues might facilitate the characterization of their role in the protein function.

Nuclear magnetic resonance (NMR) is a valuable experimental technique uniquely suited for high-resolution studies of disorder in proteins.[13] However, amide-proton-detected NMR experiments commonly used for protein studies are hindered in the characterization of intrinsically disordered proteins due to poor resonance dispersion and fast exchange of amides with water limiting the observation of complete set of resonances. This can be partly circumvented by experiments with Hα-detection.[14] To the contrary, NMR experiments directly detecting ^{13}C overcome these limitations as the random coil carbon chemical shifts have greater dispersion than proton chemical shifts, and observation of ^{13}C is not affected by exchange of amide protons with water.[15] Additional advantages of carbon-detected experiments include the observation of resonances corresponding to the backbone Cα and C′ carbons allowing for the detection of all amino acids, including proline, which is frequently found in disordered regions.[16] The use of ^{13}C-detected experiments for the analysis of the disordered proteins α-synuclein,[17] the N-terminal of c-Src kinase,[18] and β-2-microglobulin[19] at neutral pHs and ambient temperatures demonstrates the advantages of these experiments for systems where H-D exchange broadening limits the utility of proton-detected experiments. Furthermore, we have previously shown that ^{13}C-detected experiments can be used to characterize protein–protein interactions involving disordered proteins.[20]

Here, we demonstrate that ^{13}C-based NMR techniques provide a very efficient approach to characterize disordered regions within large, globular proteins. We find that this method allows for the detection of long-disordered regions as well as the highly accurate identification of even relatively short-disordered fragments (~10 amino acids long). We used ^{13}C-detected experiments to identify such disordered regions in menin. Menin is a tumor suppressor protein that controls cellular growth in endocrine tissues[21] and also functions as an oncogenic cofactor required for leukemogenesis.[22] Structural studies were recently undertaken, and while full-length menin proved to be recalcitrant to crystallization experiments, successful crystallization of the protein was achieved through the deletion of internal-disordered fragments.[23,24] The first menin to be crystallized was the homolog from *Nematostella vectensis*, and crystallization required truncation of the C-terminus and deletion of one internal-disordered fragment.[23] More recently, human menin was crystallized, also requiring the deletion of a long internal fragment predicted to be unstructured.[24] We evaluated whether these internal-disordered fragments could be identified through ^{13}C-detected NMR experiments. As model proteins, we chose C-terminally truncated constructs of *Nematostella* menin (*N*_meninΔC corresponding to residues 1–468) and human menin with the partial deletion of an internal fragment and truncation of the C-terminus (*H*_meninΔΔC corresponding to residues 1–593 with the deletion of residues 465–524). Such truncated proteins were selected to achieve soluble protein while retaining significant molecular weight.

Results and Discussion

Sequence analysis using the DISOPRED2 server[3] revealed that all menin homologs have multiple internal regions predicted to be disordered. We first tested whether ^{13}C-NMR experiments could be used to identify these internal-disordered fragments in *Nematostella* menin. The CACO spectrum of ^{13}C,^{15}N-labeled *N*_meninΔC revealed the presence of ~27 resonances [Fig. 1(A)]. Given the significant molecular weight of the protein (55 kDa), we expect that all observable signals correspond to the most disordered residues. Slow tumbling of the protein molecule leads to very strong broadening of resonances for structured fragments and acts as an efficient filter leaving observable signals only for highly mobile residues. To assign these observed resonances, we also collected CBCACO and CANCO experiments.[25,26] Through sequential assignment, we found that the majority of these signals correspond to an internal fragment (residues 423–440), 5 N-terminal residues and 2 C-terminal residues [Fig. 1(A)]. We found that analysis of Cβ-C′ correlations was essential for the assignment due to less significant peak overlap in this region and because the Cβ chemical shifts allow for the identification of the amino acid type [Fig. 1(B) and Supporting Information Fig. 1]. We were not able to assign several remaining peaks due to reduced intensities. Most likely, these peaks correspond to the shorter and less-disordered loops. The assigned residues 423–440 yield strong resonances, clearly indicating that this fragment is disordered in solution. Consistently, deletion of residues 426–442 in *Nematostella* menin was necessary to obtain diffraction quality crystals and to determine the X-ray structure of the protein.[23] We also assessed whether disordered fragments can be identified using standard amide-proton-detected experiments. The ^{1}H-^{15}N heteronuclear single quantum coherence (HSQC) spectrum for *N*_meninΔC at pH 7.5 reveals the presence of ~20–25 peaks for backbone amides including the number of strongly broadened resonances (Supporting Information Fig. 2). This indicates that ^{13}C detection

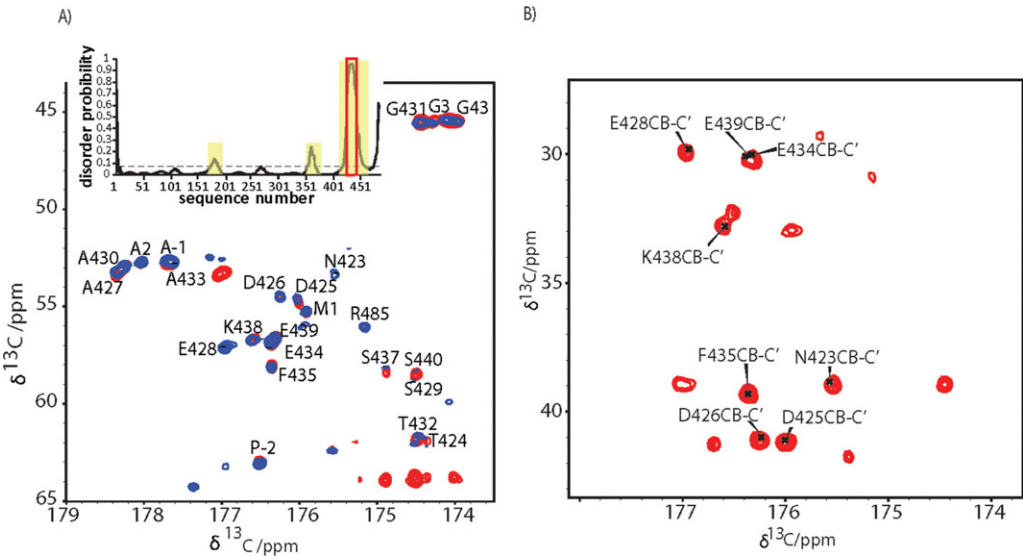

Figure 1. Assignment of disordered residues in *Nematostella* menin. A: 2D 13C CACO (blue) and CBCACO (red) NMR spectra for $^{13}C,^{15}N$ N_meninΔC. Insert shows disorder prediction from the DISOPRED2 server[3] for this construct. Dashed line shows the threshold for predicted disordered regions (highlighted in yellow). Red box indicates the experimentally observed disordered fragment of the protein. B: 2D^{13}C CBCACO NMR spectrum for $^{13}C,^{15}N$ N_meninΔC showing peak dispersion and signature chemical shifts of Cβ-C′ correlations in the fragment 422–442.

yields a clear benefit to identify disordered fragments as these spectra are not affected by the H–D exchange phenomenon.

The internal-disordered fragment in *Nematostella* menin is fairly short, and its assignment based on ^{13}C-detected experiments was relatively

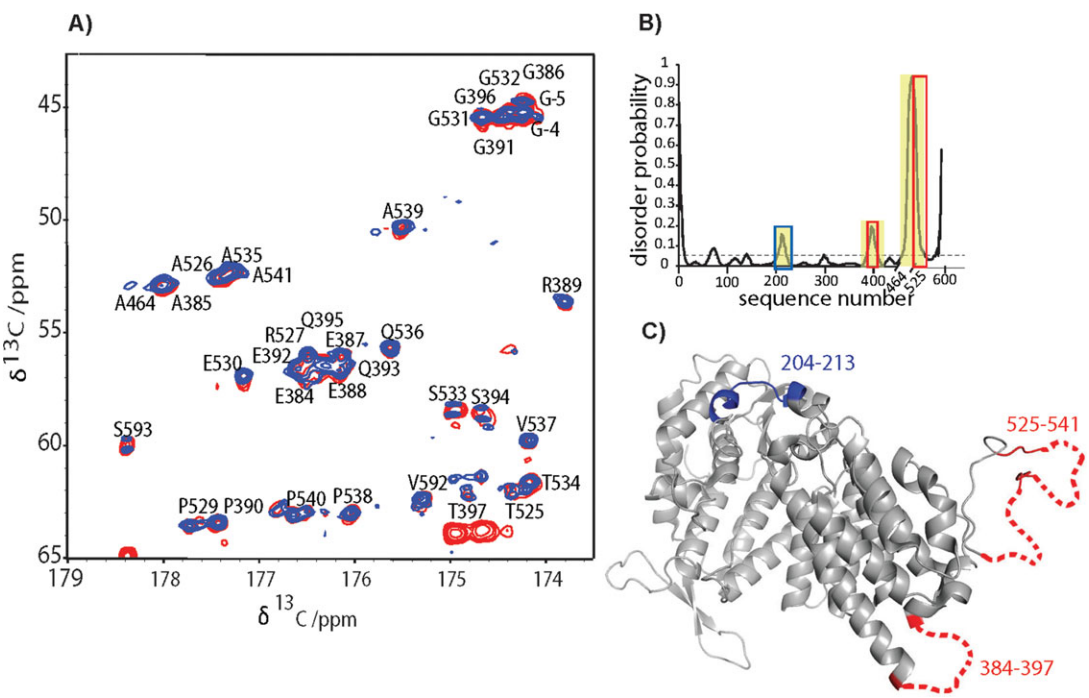

Figure 2. Assignment of disordered regions in human menin. A: 2D ^{13}C CACO (blue) and CBCACO (red) NMR spectra for $^{13}C,^{15}N$ H_meninΔΔC are shown with the assignment. B: Disorder prediction from the DISOPRED2 server[3] for the H_meninΔΔC construct. The predicted disordered regions are highlighted in yellow. Experimentally observed disordered fragments are boxed in red, and the well-ordered fragment is boxed in blue. C: Crystal structure of human menin[24] showing disordered fragments observed in ^{13}C-detected NMR experiments (red). Predicted disordered residues 204–213 (blue) belong to a structured loop within the protein.

straightforward. However, unambiguous assignment for more complex proteins with multiple-disordered fragments would be more difficult due to increased peak overlap and complexity of the 2D spectra. Therefore, we assessed whether assignment of disordered regions based on ^{13}C experiments could be facilitated by combining bioinformatics methods for disorder prediction and chemical shift calculation. To test this, we first used the program DISOPRED2[3] for the prediction of internal regions of increased disorder in *N*_meninΔC. Based on this method, three possible internal-disordered regions were identified: residues 177–187, 356–367, and 418–456 [Fig. 1(A), inset]. We next assumed that these disordered fragments would have chemical shifts consistent with random-coil values, which can be predicted with high accuracy.[27–29] Thus, we used the ncIDP program[27] to generate predicted chemical shifts for these regions. These predicted chemical shifts were used to simulate spectra with Cβ-C′, Cα-C′, and C'_i-$C\alpha_{i+1}$ correlations and compared to experimental data for *N*_meninΔC. Using this approach, we found that observed resonances correspond to residues 423–440, consistent with the manual assignment. Overall, this analysis validated the use of chemical shift prediction as a very efficient strategy to aid in completing the assignment of disordered regions in large proteins.

We next applied this strategy to assign unstructured fragments in human menin, which represents a more complex protein. The CACO and CBCACO experiments measured for *H*_meninΔΔC indicated the presence of 34 disordered residues with more significant overlap compared to the *N*_meninΔC spectra [Fig. 2(A)]. The unambiguous assignment of these residues based on the combination of CACO, CBCACO, and CANCO experiments was difficult due to extensive signal overlap. To aid in the assignment of these resonances, we carried out chemical shift prediction for the fragments with the highest disorder probability. Analysis of the *H*_meninΔΔC sequence using the DISOPRED2 program identified three potential disordered regions: 204–213, 383–401, and 457–549 [Fig. 2(B)].

Using chemical shift prediction in conjunction with ^{13}C-detected experiments acquired for sequential assignment, we unambiguously assigned two internal regions corresponding to residues 384–397 and 525–541. As observed for *Nematostella* menin, we also detected several additional peaks, corresponding to two N-terminal and two C-terminal residues in *H*_meninΔΔC. The longest disordered fragment, which we assigned, residues 525–541, was also predicted with high probability using the DISOPRED2 server [Fig. 2(B)]. These residues are unstructured in the recently reported crystal structure of human menin[24] with only a short fragment observed due to crystal packing interactions [Fig. 2(C)]. We also found that of the two remaining fragments predicted with lower confidence to be disordered, only residues 384–397 are disordered in solution. This is consistent with the crystal structure of human menin, which is lacking electron density for residues 386–402 [Fig. 2(C)].[24] To the contrary, the second fragment encompassing residues 204–213 predicted to be disordered was not detected in ^{13}C-NMR experiments, and, indeed, this region is well ordered in the crystal structure of human menin [Fig. 2(C) and Supporting Information Figs. S3 and S4].[24]

As expected, we observed very good correlations between predicted and experimentally assigned chemical shifts for all resonances detected on menin spectra. The root-mean-square deviation (RMSD) values for the *Nematostella* menin are 0.21, 0.19, and 0.28 ppm for Cα, Cβ, and C′ chemical shifts, respectively. The RMSD between predicted and experimental chemical shifts for human menin is 0.34 for Cα, 0.18 for Cβ, and 0.30 ppm for C′ chemical shifts. Such close agreement demonstrates that chemical shift predication provided a very valuable tool for the rapid assignment of the spectra even in the presence of strong spectral overlap. We anticipate that the combination of ^{13}C-detected experiments with chemical shift predication will be highly beneficial for rapid assignment of even more complex spectra with longer disordered fragments.

We expected that an important advantage of ^{13}C-detected experiments over detection of amide protons is the possibility to record spectra at a broad pH range without compromising the number of observed signals. To assess this, we tested the effect of pH on the spectra of the *H*_meninΔΔC protein (Fig. 3). As expected, the number of backbone amide signals in ^{1}H-^{15}N HSQC spectra increased dramatically with decreasing pH. At pH 8.5, we observed only approximately five to seven sharp peaks, while by lowering the pH to 7.5 and 6.5, we observed, respectively, 15–18 and 30–32 sharp peaks. Even at the lowest pH, a number of peaks remained broad, which would most likely limit the assignment based on the HN-detected triple-resonance experiments. The CACO and CBCACO spectra at this range of pHs consistently showed ~34 peaks, which would allow for complete assignment of disordered residues under a broad range of pHs. Importantly, we have recorded high-quality ^{13}C experiments for protein concentration as low as 50 μ*M* demonstrating applicability of this approach to large proteins with low solubility or particular buffer requirements.

In summary, we have developed a simple method for the identification and assignment of disordered regions in large proteins. We have demonstrated that (1) the use of carbon-detected NMR experiments allows for the identification of disordered residues in two homologs of menin (each protein is larger than 50 kDa); (2) this method allows

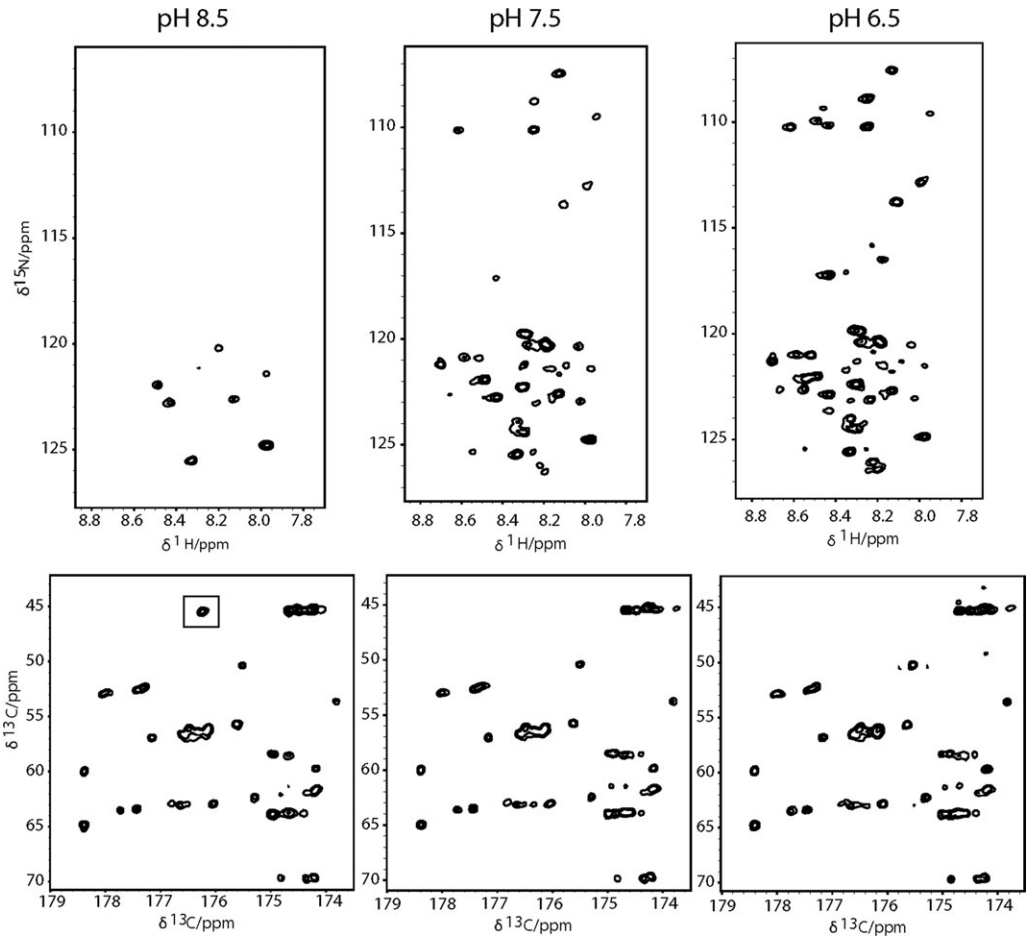

Figure 3. Effect of pH on the number of observed backbone resonances in HN- and ^{13}C-detected experiments. Top: ^{1}H-^{15}N HSQC experiments for 50 μ*M H*_meninΔΔC at pH 8.5 (left), 7.5 (center), and 6.5 (right). The fragment of the HSQC spectra showing side-chain amides is omitted for clarity. Bottom: CBCACO spectra recorded for the same samples as mentioned earlier showing 34 backbone peaks at entire range of pHs. The C′ chemical shift of the N-terminal glycine (boxed) is pH-dependent and is downfield shifted at pH 8.5 compared to spectra at other pHs.

for the complete detection of disordered residues at broad range of pHs when compared with standard amide-proton-detected experiments; (3) high-quality ^{13}C experiments can be recorded at low (∼50–100 μ*M*)-protein concentrations; (4) the assignment of relatively complex spectra can be rapidly achieved through the combination of experimental data with chemical shift calculation. Importantly, the NMR experiments allowed for highly accurate identification of even relatively short disordered fragments (∼10 amino acid long), which are more difficult to predict using bioinformatics methods.[6] We have also demonstrated that the fragment of *Nematostella* menin, which was previously deleted for protein crystallization,[23] is disordered in solution. Therefore, identification of disordered internal fragments through this method may serve to strongly support optimization of constructs for protein crystallization. Indeed, we have very recently used this approach to support engineering of a construct of human menin and obtained high-quality crystals diffracting to 1.3–1.5 Å resolution.[30] Such an NMR-based approach is complementary to the high-resolution deuterium exchange mass spectroscopy (DXMS) method, which is frequently used for the detection of disordered fragments in proteins and construct optimization.[11,12,31] Contrary to DXMS, NMR spectroscopy provides direct information regarding backbone flexibility and might be more suitable to distinguish disordered fragments from solvent-exposed and structured loops. Additionally, the direct high-resolution observation of disordered regions in large proteins using ^{13}C-detected NMR may support future characterization of these regions as functional components of globular proteins.

Materials and Methods

Protein purification

The synthetic construct encoding *Nematostella* menin was ordered from GenScript and cloned into the pET32a vector. The truncation after residue 487 led to the generation of the *N*_meninΔC, which was used for NMR experiments. The ^{13}C,^{15}N-labeled

*N*_meninΔC protein was expressed by growing bacterial cells in isotopically enriched M9 minimal media. The purification was carried out following previously described protocol.[23]

The synthetic gene encoding human menin with an internal deletion (Δ465–524) was ordered from GenScript and subcloned into pET32a vector (Novagen). The construct *H*_meninΔΔC was made by introducing stop codon to generate truncation following residue 593. *H*_meninΔΔC was expressed in Rosetta2(DE3) cells (Novagen) grown in isotopically enriched M9 minimal media and purified using affinity chromatography column HisTrap HP (GE Healthcare) followed by ion exchange using Q Sepharose FF (GE Healthcare). To remove the thioredoxin-His6 tag, the protein was cleaved by TEV protease and loaded onto Ni-NTA superflow resin (Qiagen). The protein was further purified by size exclusion chromatography using HiLoad 16/60 Superdex 75 pg (GE Healthcare).

NMR spectroscopy

For NMR experiments, the ^{13}C,^{15}N-labeled *N*_meninΔC sample was prepared at a final concentration of 100 μ*M* in 50 m*M* Tris buffer, pH 7.5, 150 m*M* NaCl, and 1 m*M* tris(2-carboxyethyl)phosphine (TCEP) with 10% D_2O. The ^{13}C,^{15}N-labeled *H*_meninΔΔC sample was prepared to a final concentration of 115 μ*M* in 50 m*M* Tris, pH 7.5, 50 m*M* NaCl, and 1 m*M* dithiothreitol (DTT) with 10% D_2O. pH titration experiments were prepared at 50 μ*M* in 50 m*M* Tris, pH 6.5/7.5/8.5, 50 m*M* NaCl, and 1 m*M* dithiothreitol (DTT) with 10% D_2O. NMR measurements were performed using a Bruker Advance III 600-MHz spectrometer equipped with 5-mm TCI cryogenic probe. The following parameters were used for ^{13}C-detected experiments: 2D CACO[25] data size: 64 (t_1) × 512 (t_2) complex points, t_{1max} (^{13}C) = 16 ms, and t_{2max} (^{13}C) = 85.2 ms; 2D CBCACO[25] data size: 70 (t_1) × 512 (t_2) complex points, t_{1max} (^{13}C) = 7.8 ms, and t_{2max} (^{13}C) = 85.2 ms; 2D CANCO[26] data size 50 (t_1) × 512 (t_2) complex points, t_{1max} (^{13}C) = 7.4 ms, and t_{2max} (^{13}C) = 85.2 ms. All ^{13}C-detected experiments were recorded with ^{1}H excitation in order to increase the sensitivity and processed with the in-phase anti-phase (IPAP) scheme for decoupling. These experiments were recorded with 1-s relaxation delay and 32, 64, and 448 scans per increment, respectively. This led to total acquisition times of 2.5, 6, and 31 h. All experiments were collected at 25°C. Spectra were processed with NMRPipe[32] and analyzed with Sparky (http://www.cgl.ucsf.edu/home/sparky/).

References

1. Dyson HJ, Wright PE (2005) Intrinsically unstructured proteins and their functions. Nat Rev Chem Biol 6: 197–208.
2. Dunker AK, Brown CJ, Lawson JD, Iakoucheva LM, Obradovic Z (2002) Intrinsic disorder and protein function. Biochemistry 41:6573–6582.
3. Ward JJ, Sodhi JS, McGuffin LJ, Buxton BF, Jones DT (2004) Prediction and functional analysis of native disorder in proteins from the three kingdoms of life. J Mol Biol 337:635–645.
4. Wang RY, Han Y, Krassovsky K, Sheffler W, Tyka M, Baker D (2011) Modeling disordered regions in proteins using Rosetta. PloS One 6:e22060.
5. Bordoli L, Kiefer F, Schwede T (2007) Assessment of disorder predictions in CASP7. Proteins 69:129–136.
6. He B, Wang K, Liu Y, Xue B, Uversky VN, Dunker AK (2009) Predicting intrinsic disorder in proteins: an overview. Cell Res 19:929–949.
7. Deng X, Eickholt J, Cheng J (2012) A comprehensive overview of computational protein disorder prediction methods. Mol BioSyst 8:114–121.
8. Li X, Wang J, Shi Y (2011) Structural mechanisms of DIAP1 auto-inhibition and DIAP1-mediated inhibition of drICE. Nat Commun 2:408.
9. Chen GQ, Sun Y, Jin R, Gouaux E (1998) Probing the ligand binding domain of the GluR2 receptor by proteolysis and deletion mutagenesis defines domain boundaries and yields a crystallizable construct. Protein Sci 7:2623–2630.
10. Armstrong N, Sun Y, Chen GQ, Gouaux E (1998) Structure of a glutamate-receptor ligand-binding core in complex with kainate. Nature 395:913–917.
11. Pantazatos D, Kim JS, Klock HE, Stevens RC, Wilson IA, Lesley SA, Woods VL Jr (2004) Rapid refinement of crystallographic protein construct definition employing enhanced hydrogen/deuterium exchange MS. Proc Natl Acad Sci USA 101:751–756.
12. Sharma S, Zheng H, Huang YJ, Ertekin A, Hamuro Y, Rossi P, Tejero R, Acton TB, Xiao R, Jiang M, Zhao L, Ma LC, Swapna GV, Aramini JM, Montelione GT (2009) Construct optimization for protein NMR structure analysis using amide hydrogen/deuterium exchange mass spectrometry. Proteins 76:882–894.
13. Dyson JH, Wright PE (2004) Unfolded proteins and protein folding studied by NMR. Chem Rev 104: 3607–3622.
14. Mäntylahti S, Hellman M, Permi P (2011) Extension of the HA-detection based approach: (HCA)CON(CA)H and (HCA)NCO(CA)H experiments for the main-chain assignment of intrinsically disordered proteins. J Biomol NMR 49:99–109.
15. Felli IC, Pierattelli R (2012) Recent progress in NMR spectroscopy: toward the study of intrinsically disordered proteins of increasing size and complexity. IUBMB Life 64:473–481.
16. Bermel W, Bertini I, Felli IC, Lee YM, Luchinat C, Pierattelli R (2006) Protonless NMR experiments for sequence-specific backbone nuclei in unfolded proteins. J Am Chem Soc 128:3918–3919.
17. Hsu ST, Bertoncini CW, Dobson CM (2009) Use of protonless NMR spectroscopy to alleviate the loss of information resulting from exchange-broadening. J Am Chem Soc 131:7222–7223.
18. Pérez Y, Gairí M, Pons M, Bernadó P (2009) Structural characterization of the natively unfolded N-terminal domain of human c-Src kinase: insights into the role of phosphorylation of the unique domain. J Mol Biol 391: 136–148.
19. Skora L, Becker S, Zweckstetter M (2010) Molten globule precursor states are conformationally correlated to amyloid fibrils of human beta-2-microglobulin. J Am Chem Soc 132:9223–9225.

20. Grembecka J, Belcher AM, Hartley T, Cierpicki T (2010) Molecular basis of the mixed lineage leukemia-menin interaction: implications for targeting mixed lineage leukemias. J Biol Chem 285:40690–40698.
21. Chandrasekharappa SC, Guru SC, Manickam P, Olufemi SE, Collins FS, Emmert-Buck MR, Debelenko LV, Zhuang Z, Lubensky IA, Liotta LA, Crabtree JS, Wang Y, Roe BA, Weisemann J, Boguski MS, Agarwal SK, Kester MB, Kim YS, Heppner C, Dong Q, Spiegel AM, Burns AL, Marx SJ (1997) Positional cloning of the gene for multiple endocrine neoplasia-type 1. Science 276:404–407.
22. Yokoyama A, Somervaille TC, Smith KS, Rozenblatt-Rosen O, Meyerson M, Cleary ML (2005) The menin tumor suppressor protein is an essential oncogenic cofactor for MLL-associated leukemogenesis. Cell 123: 207–218.
23. Murai MJ, Chruszcz M, Reddy G, Grembecka J, Cierpicki T (2011) Crystal structure of menin reveals binding site for mixed lineage leukemia (MLL) protein. J Biol Chem 286:31742–31748.
24. Huang J, Gurung B, Wan B, Matkar S, Veniaminova NA, Wan K, Merchant JL, Hua X, Lei M (2012) The same pocket in menin binds both MLL and JunD but has opposite effect on transcription. Nature 482: 542–546.
25. Bermel W, Bertini I, Duma L, Felli IC, Emsley L, Pierattelli R, Vasos PR (2005) Complete assignment of heteronuclear protein resonances by protonless NMR spectroscopy. Angew Chem Int Ed Engl 44:3089–3092.
26. Bermel W, Bertini I, Felli IC, Pierattelli R, Vasos PR (2005) A selective experiment for the sequential protein backbone assignment from 3D heteronuclear spectra. J Mag Res 172:324–328.
27. Tamiola K, Acar B, Mulder FA (2010) Sequence-specific random coil chemical shifts of intrinsically disordered proteins. J Am Chem Soc 132:18000–18003.
28. Schwarzinger S, Kroon GJ, Foss TR, Chung J, Wright PE, Dyson HJ (2001) Sequence-dependent correction of random coil NMR chemical shifts. J Am Chem Soc 123: 2970–2978.
29. Wang Y, Jardetzky O (2002) Probability-based protein secondary structure identification using combined NMR chemical-shift data. Protein Sci 11:852–861.
30. Shi A, Murai MJ, He S, Lund G, Hartley T, Purohit T, Reedy G, Chruszcz M, Grembecka J, Cierpicki T (in press) Structural insights into inhibition of the bivalent menin-MLL interaction by small molecules in leukemia. Blood; e-pub: blood-2012-05-429274v1.
31. Spraggon G, Pantazatos D, Klock HE, Wilson IA, Woods VL Jr, Lesley SA (2004) On the use of DXMS to produce more crystallizable proteins: structures of the *T. maritima* proteins TM0160 and TM1171. Protein Sci 13:3187–3199.
32. Delaglio F, Grzesiek S, Vuister GW, Zhu G, Pfeifer J, Bax A (1995) NMRPipe: a multidimensional spectral processing system based on UNIX pipes. J Biomol NMR 6:277–293.